River Flow 2014 – Schleiss et al. (Eds)
© 2014 Taylor & Francis Group, London, ISBN 978-1-138-02674-2

A numerical calculation method for flow in the presence of isolated boulders atop a rough bed by using an enhanced depth integrated model with a non-equilibrium resistance law

T. Uchida & S. Fukuoka
Research and Development Initiative, Chuo University, Japan

A.N. Papanicolaou & A.G. Tsakiris
IIHR-Hydroscience and Engineering, The University of Iowa, USA

ABSTRACT: This paper presents a new calculation method for flow over rough bed with a superimposed array of wall-mounted boulders. Since the resistance of roughness depends on the relative water depth to roughness height for the case of Large Scale Roughness (LSR), it is necessary for calculating the flow over gravel bed rivers to separate the effects of LSR from that of the Small Scale Roughness (SSR). A quasi-3D calculation method (BVC method) is developed to evaluate velocity vertical distributions around boulders without making the shallow water assumption. To evaluate additional resistance on rough bed resulted from the increment in momentum exchange due to flow around boulders, a non-equilibrium wall law is proposed and the bottom vortex layer and roughness layer equations are derived. The advantages of BVC method with the non-equilibrium wall law over the 2D and BVC method with the conventional equilibrium wall law are demonstrated through comparisons with benchmark experimental results.

1 INTRODUCTION

The presence of isolated large roughness such as boulders or clusters in gravel bed rivers, which in some instances may even protrude through the free surface, produces challenging conditions for determining near-bed flow conditions and flow resistance. Many researchers have indicated that the conventional wall law is inadequate when the large roughness element diameter is comparable to the water depth (Bathurst, 1985; Aguirre-Pe & Fuentes, 1990; Clifford et al., 1992, Katul et al., 2002). Recently, Computational Fluid Dynamics (CFD) has been widely used to evaluate flows in gravel bed rivers (Olsen & Stokseth 1995; Nicholas, 2001; Carney et al., 2006; Nikora et al., 2007a, 2007b; Rameshwaran et al., 2011). Since the resistance of roughness depends on the relative water depth to roughness height for the case of Large Scale Roughness (LSR), the concept of the roughness scale distinction, or multi-scale roughness, in which the effects of LSR is separated from that of the Small Scale Roughness (SSR), has been proposed by many researchers (Clifford et al., 1992; Nicholas, 2001; Carney et al., 2006; Rameshwaran et al., 2011). Yet some important issues still remain unresolved.

The first issue is an evaluation method of LSR. While we recognize the need of a non-hydrostatic three dimensional method for this purpose (Olsen & Stokseth 1995; Nicholas, 2001; Carney et al., 2006; Nikora et al., 2007a, 2007b; Rameshwaran et al., 2011), a reliable depth integrated model is also required for practical applications to rivers. However, previous depth integrated models including quasi-three dimensional models cannot be used in this case, because of their hydrostatic pressure distribution assumption (Ishikawa et al., 1986; Fukuoka et al., 1992; Jin & Steffler 1993; Yeh and Kennedy, 1993). The second issue is the effects of LSR on SSR. The applicability of the conventional wall law for rough bed (log-law with equivalent roughness) is uncertain because the near bed flow is affected by the LSR presence. For flows over a gravel bed, the existence of boulders and the irregularity of the bed topography and sediment diameter exacerbate the deviations from an equilibrium bottom boundary condition. The essential solution is to calculate the non-equilibrium motion around bed surface including the roughness layer (Olsen and Stokseth, 1995; Lane et al., 2004; Carney et al., 2006; Nicora et al., 2007a, 2007b; Rameshwaran et al., 2011).

Recently, we have developed a new quasi-three dimensional calculation method that avoids making shallow water assumptions, such as hydrostatic pressure distribution, the general Bottom Velocity Computation (BVC) method, in which the equations for velocity and pressure distributions

in the vertical direction are solved with depth averaged velocity equations (Uchida & Fukuoka, 2012). The BVC method has been validated for several flows including rapidly varied flows over a structure and three dimensional flows around a non-submerged structure where the horseshoe vortex is prominent (Uchida & Fukuoka, 2012, 2013; Fukuoka & Uchida, 2013). However, the applicability of the BVC method for evaluating the effects of submerged boulders as LSR has not been discussed. In addition, the previous BVC method has employed the conventional equilibrium wall law without considering the effect of LSR on SSR. This paper proposes the improved BVC method to employ a non-equilibrium wall law by introducing momentum equations for the bottom vortex layer and roughness layer. The validity of the present method is discussed through comparisons with experimentally measured velocity distributions in within an array of isolated boulders atop a rough bed and with calculated results from the 2D and BVC with the conventional equilibrium wall law methods.

2 CALCULATION METHOD

2.1 *Representation of multi-scale roughness and the framework of the BVC method*

In the present calculation method, the roughness is divided into Large Scale Roughness (LSR), which includes boulders with comparable height to the water depth that may even protrude through the free surface, and Small Size Roughness (SSR), the contributions of which are evaluated using the wall law. The LSR is explicitly taken into account in the flow calculation as variation in bed topography as indicated in Figure 1. The BVC method (Uchida and Fukuoka, 2011) is refined to calculate fluid flow and evaluate the effects of LSR directly, newly introducing momentum and vorticity exchange owing to those fluxes on bed. The BVC method is a quasi-three dimensional calculation method without the need to make key shallow water assumptions, such as the hydrostatic pressure distribution assumption, in which equations for velocity and pressure distributions in vertical direction are solved with depth averaged velocity equations as described below.

The BVC method considers the thin vortex layer δz_b on bed surface and calculates the bottom velocity acting on the layer as shown in Figure 2. The bottom equations are derived by depth-integrating the horizontal vorticity:

$$u_{bi} = u_{si} - \varepsilon_{ij3}\Omega_j h - \left(\frac{\partial Wh}{\partial x_i} - w_s \frac{\partial z_s}{\partial x_i} + w_b \frac{\partial z_b}{\partial x_i} \right) \quad (1)$$

where, i, j = 1(x), 2(y) (x,y: horizontal direction, z: vertical direction), u_{bi}: bottom velocity, u_{si}: water surface velocity, ε_{ijk}: Levi-Civita symbol, Ω_j: Depth Averaged (DA) horizontal vorticity, h: water depth, W: DA vertical velocity, z_s: water level, z_b: bed level, w_s, w_b: vertical velocity on water surface and bottom. Equation (1) implies that the bottom velocity on the thin vortex layer on the bed can be evaluated once the water surface velocity, horizontal vorticity integrated over water depth, and spatial variation in vertical velocity are known. The equations for these unknown variables are derived in the BVC method considering the cubic vertical velocity equation (2).

$$u'_i = \Delta u_i(12\eta^3 - 12\eta^2 + 1) + \delta u_i(-4\eta^3 + 3\eta^2) \quad (2)$$

where, $u'_i = u_i - U_i$, U_i: depth averaged velocity, δu_i: $u_{si} - u_{bi}$, Δu_i: $u_{si} - U_i$, $\eta = (z_s - z)/h$. The quadric curve of velocity distributions are used for the uniform

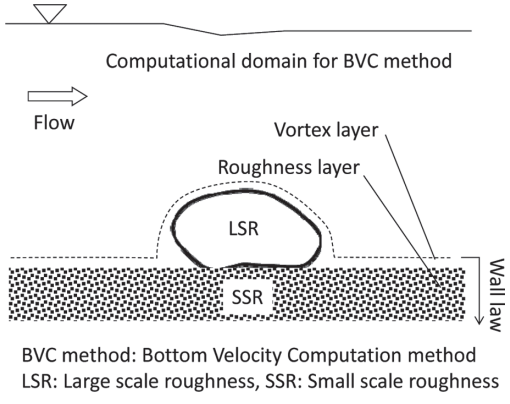

Figure 1. Representation of multi-scale roughness.

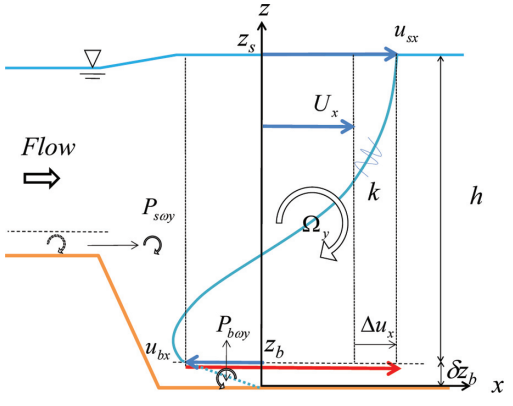

Figure 2. BVC method.

flow, substituting $\Delta u_i = \delta u_i/3$ ($u_{sei} = U_i + \delta u_i/3$) in the equation (2) (Uchida & Fukuoka, 2011). On the other hand, the bottom pressure deviation from the hydrostatic pressure distribution is given by depth-integrating the vertical momentum equation after neglecting the temporal variation term for computational stability and simplicity.

$$\frac{dp_b}{\rho} = \frac{\partial hWU_j}{\partial x_j} + \tau_{bj}\frac{\partial z_b}{\partial x_j} - \frac{\partial h\tau_{zj}}{\partial x_j} \tag{3}$$

where, dp: pressure deviation from hydrostatic pressure distribution ($p = \rho g(z_s - z) + dp$), dp_b: dp on the bottom, τ_{ij}: shear stress tensor due to molecular and turbulence motions.

To calculate Eqs. (1) and (3), the governing equations for the following unknown quantities are solved: water depth h (Eq. (4)), DA horizontal velocity U_i (Eq. (5)), DA turbulence energy k (Eq. (6)), DA horizontal vorticity Ω_i, (Eq. (7)) horizontal velocity on water surface u_{si} (Eq. (8)), DA vertical velocity W (Eq. (9)).

$$\frac{\partial h}{\partial t} + \frac{\partial U_j h}{\partial x_j} - w_{\sigma b} = 0 \tag{4}$$

$$\frac{\partial U_i h}{\partial t} + \frac{\partial U_i U_j h}{\partial x_j} - w_{\sigma b}u_{bi} = -gh\frac{\partial z_s}{\partial x_i} - \frac{\tau_{bi}}{\rho} + \frac{\partial hT_{ij}}{\rho \partial x_j} - \left(\frac{\partial h dp_0}{\rho \partial x_i} + \frac{dp_b}{\rho}\frac{\partial z_b}{\partial x_i}\right) \tag{5}$$

$$\frac{\partial k}{\partial t} + U_j\frac{\partial k}{\partial x_j} = \frac{1}{h}\frac{\partial}{\partial x_i}\left(\frac{\nu h}{\sigma_k}\frac{\partial k}{\partial x_i}\right) + P_k - \varepsilon \tag{6}$$

$$\frac{\partial \Omega_i h}{\partial t} = R_{\sigma i} + P_{\omega i} + \frac{\partial hD_{\omega ij}}{\partial x_j} + w_{\sigma b}\omega_{bi} \tag{7}$$

$$\frac{\partial u_{si}}{\partial t} + u_{sj}\frac{\partial u_{si}}{\partial x_j} = -\left\{g + \left(\frac{\partial dp}{\partial z}\right)_{z=z_s}\right\}\frac{\partial z_s}{\partial x_i} + P_{si} \tag{8}$$

$$\frac{\partial}{\partial x_j}\left((C\Delta t)^2\frac{\partial \phi}{\partial x_j}\right) + \phi^P - \phi = 0 \tag{9}$$

where, $w_{\sigma b}$: velocity flux across the bottom layer as described in the following section ($w_{\sigma b} = 0$: equilibrium wall law), $T_{ij} = \overline{\tau_{ij} + u_i' u_j'}$ (superscript bar indicates depth averaged value and evaluated by vertical velocity distribution), $\tau_{ij} = \nu S_{ij}$, $\nu = \nu_m + \nu_t$, ν_m: kinematic viscosity coefficient, ν_t: kinematic eddy viscosity coefficient, S_{ij}: DA strain velocity, dp_0: DA pressure deviation evaluated as $dp_0 = dp_b/2$ with the assumption of the linear pressure distribution for simplicity, P_k: the production term of turbulence energy, ε: the dissipation term of turbulence energy, $R_{\sigma i}$: the rotation term of vertical vorticity ($R_{\sigma i} = u_{si}\omega_{\sigma s} - u_{bi}\omega_{\sigma b}$), $\omega_{\sigma s}$, $\omega_{\sigma b}$: rotation of u_{si}, u_{bi}, $P_{\omega i}$: the production term of horizontal vorticity, $D_{\omega ij}$: horizontal vorticity flux due to convection, rotation, dispersion and turbulence diffusion, P_{si}: the production term of surface velocity (shear stress under the water surface layer), $C = k_1 h/\Delta t$, $k_1 = 1/20$, $\phi = (Wh)^{n+1} - (Wh)^n$, $\phi^P = (Wh)^P - (Wh)^n$, $(Wh)^P$: the predicted Wh calculated by the continuity equation using $(\delta u_i)^P$, $(\delta u_i)^P$: predicted velocity difference calculated by Eq. (1) with $(Wh)^n$. These equations can be solved once a vertical velocity distribution is assumed. More details on the equations and the numerical computation methods for the BVC method may be found in Uchida & Fukuoka (2011, 2012 and 2013).

2.2 *Equilibrium bottom boundary conditions*

Boundary conditions on the bottom for the bed shear stress terms in momentum equations (5) and the production terms in vorticity equations (7) can be derived from the wall law for the rough bed. According to the logarithmic law for flat rough bed, the relationship between friction velocity and velocity near the bed may be expressed as (Schlichting and Gersten, 2000):

$$\frac{u_b}{u_*} = c_b = \frac{1}{\kappa}\ln\left(\frac{z_b}{k_s}\right) + Ar \tag{10}$$

where, $u_b^2 = u_{bi}u_{bi}$, $z_b = \delta z_b + \delta z_0$, δz_b: very thin vortex layer assumed in the BVC method, δz_0: depth of the log law origin from the top of the roughness height. The vortex layer thickness is defined as $h/\delta z_b = e^3 - 1$ (e: base of natural logarithm) to satisfy the vertical velocity distribution simplified of equation (2) for uniform flow conditions with logarithmic velocity distribution.

The vorticity distribution is given by the differential of velocity equation (2) with respect to z. The production terms $P_{\omega i}$ in equation (7) are given by equation (11).

$$P_{\omega i} = C_{p\omega}\nu_{tb}(\omega_{bei} - \omega_{bi})/h + P_{s\omega i} \tag{11}$$

where, $C_{p\omega} = \kappa/\alpha$, ν_{tb}: ν_t on the bottom converted into depth averaged scale, ω_{bi}: horizontal vorticity on bottom, ω_{bei}: equilibrium ω_{bi}, $P_{s\omega i}$: vorticity production due to flow separation (Uchida & Fukuoka, 2011, 2013). The equivalent vorticity on the bottom is twice of that of the depth averaged value $\omega_{be} = 2\Omega_e = 2\delta u_e/h$. Equation (12) gives the equilibrium vorticity on the bottom (Uchida & Fukuoka, 2011):

$$\omega_{be} = \frac{2u_*}{\kappa h}\ln\left(\frac{z_s}{z_b}\right) \tag{12}$$

2.3 *Non-equilibrium bottom boundary conditions*

An issue with the equilibrium bottom boundary condition is the assumption of uniform flow condition for a bottom velocity regardless of the velocity and vorticity distributions above the bottom. For example, the same velocity distribution for vortex and roughness layer is assumed for different velocity distributions above the bottom (solid and dotted lines of velocity vertical distributions in BVC calculation layer in Fig. 3). This study defines the unknown variables in the vortex and roughness layers as shown in Figure 3 to calculate non-equilibrium flow under the bottom of the BVC calculation layer. The assumption of very thin layer gives the following momentum equations for the vortex and roughness layers:

$$\frac{\partial u_{vi}}{\partial t}+u_{vk}\frac{\partial u_{vi}}{\partial x_k}=-\frac{\partial(p_b+\rho g z_b)}{\rho\partial x_i}+\frac{\tau_{bi}}{\rho\delta z_b}-\frac{\tau_{ti}}{\rho\delta z_b} \quad (13)$$

$$\frac{\partial u_{ri}}{\partial t}+u_{rk}\frac{\partial u_{ri}}{\partial x_k}=-\frac{\partial(p_b+\rho g z_b)}{\rho\partial x_i}+\frac{\tau_{ti}}{\rho\delta z_r}-\frac{D_i}{\rho\delta z_r} \quad (14)$$

where, k = 1,2,3, u_{vi}, u_{ri}: i direction velocity in the vortex and roughness layers, p_b: bottom pressure $p_b = \rho gh + dp_b$, τ_{bi}, τ_{ti}: shear stress acting on the bottom and roughness layer surface, δz_b, δz_r: the thickness of vortex and roughness layers, D_i: resistance term due to drag force acting on roughness. The shear stress acting on the lower surface of the roughness layer is neglected in equation (14). The roughness layer thickness is assumed as $\delta z_r = k_s$ in this paper. The fluxes $w_{\sigma b}$, $w_{\sigma t}$ crossing the bottom and roughness surface are calculated with the following continuity equations for vortex and roughness layers:

$$w_{\sigma b}=w_{\sigma t}-\frac{\partial\delta z_b u_{vi}}{\partial x_i},\quad w_{\sigma t}=-\frac{\partial\lambda\delta z_t u_{ri}}{\partial x_i} \quad (15)$$

where, λ: porosity in the roughness layer ($\lambda = 0.4$).

The shear stress and resistance terms in the momentum equations for vortex and roughness layers are derived by using the equilibrium wall law as follows. The shear stress acting on those layers following the Boussinesq approximation (Shlichting & Gersten, 2000) can be assumed as:

$$\frac{\tau_{bi}}{\rho}=\left(\nu_t\frac{\partial u_i}{\partial z}\right)_b=\nu_{tb}\cdot A_b\frac{(u_{bi}-u_{vi})}{h} \quad (16)$$

$$\frac{\tau_{ti}}{\rho}=\left(\nu_t\frac{\partial u_i}{\partial z}\right)_t=\nu_{tt}\cdot A_t\frac{(u_{vi}-u_{ri})}{h} \quad (17)$$

The coefficients A_b and A_t are decided to satisfy $\tau_b = \tau_t h/(h + \delta z_b) = \rho u_*^2$ ($\tau_b^2 = \tau_{bi}\tau_{bi}$, $\tau_t^2 = \tau_{ti}\tau_{ti}$) and $\nu_{tb} = \nu_{tt} = \alpha u^* h$ with the conventional logarithmic velocity vertical distribution for the equilibrium condition:

$$A_b=\frac{1}{\alpha(c_b-c_v)},\ c_v=\frac{1}{\kappa}\ln\left(\frac{\delta z_0+\delta z_b/2}{k_s}\right)+Ar \quad (18)$$

$$A_t=\frac{1}{\alpha(c_t-c_r)}\frac{h+\delta z_b}{h},\ c_t=\frac{1}{\kappa}\ln\left(\frac{\delta z_0}{k_s}\right)+Ar \quad (19)$$

where, c_r: coefficient for the ratio between the velocity in the roughness layer and shear velocity for uniform flow condition.

The kinematic eddy viscosities on the bottom and the top of the roughness layer are expressed by using the distance of the wall and velocity difference:

$$\nu_{tb}=\alpha_b\delta u_b h,\quad \delta u_b^2=(u_{bi}-u_{vi})(u_{bi}-u_{vi}) \quad (20)$$

$$\nu_{tt}=\alpha_t\delta u_t h,\quad \delta u_t^2=(u_{vi}-u_{ri})(u_{vi}-u_{ri}) \quad (21)$$

where, the coefficient a_b and a_t are given by $a_b = \alpha/(c_b - c_v)$ and $a_t = \alpha/(c_v - c_r)$ to reduce $\nu_{tb} = \nu_{tt} = \alpha u_* h$ for the equilibrium condition. However, using bottom vorticity ω_b gives another expression of the bottom kinematic eddy viscosity ν_{tb} as presented in previous research (Uchida & Fukuoka, 2011, 2013):

$$\nu_{tb}=\frac{\alpha\kappa\omega_b h^2}{2\ln(z_s/z_b)} \quad (22)$$

This study uses the average value of equation (20) and (22) for ν_{tb}.

The resistance term D_i is expressed with the assumption of the roughness layer as the one layer of spheres array and drag coefficient C_D:

$$D_i=\frac{\pi C_D}{8}\rho u_r u_{ri} \quad (23)$$

where, $u_r^2 = u_{ri}u_{ri}$, $C_D = 0.4$. By considering the equilibrium condition in equation (14), the coefficient c_r is given by equation (24).

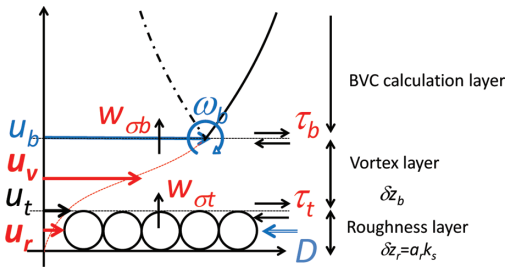

Figure 3. Calculation domains for non-equilibrium wall law.

$$c_r = \sqrt{\frac{8}{\pi C_D}\left(1+\frac{\delta z_r + \delta z_b}{h}\right)} \tag{24}$$

The equilibrium vorticity on the production term in the vorticity equation (11) is assumed by using velocity gradient in vorticity in the layer as:

$$\omega_{bej} = 2\Omega_{ej} = 2\varepsilon_{ij3} A_\omega \frac{u_{bi} - u_{vi}}{h} \tag{25}$$

where, the coefficient A_ω is obtained to reduce equation (25) to equation (12) for the equilibrium condition.

$$A_\omega = \frac{1}{\kappa(c_b - c_r)} \ln\left(\frac{z_s}{z_b}\right) \tag{26}$$

3 CALCULATION CONDITION

The conditions for the benchmark experimental results are described in the following. The experiments were conducted in a 21.0 m long, 0.91 m wide and 0.53 m deep channel with slope $S = 0.003$ by Papanicolaou et al. (2012). Three layers of glass beads with diameter $d_0 = 0.0191$ m were placed in a fixed, well-packed arrangement on the bottom. 48 immobile, spherical boulders with diameter $d_c = 0.055$ m were fixed in a staggered arrangement atop the flat porous bed of the glass beads. The diagonal spacing between boulders was $l = 6d_c$ to establish isolated roughness conditions often found in natural mountainous streams (Fig. 4). The experiment was conducted for fully submerged condition $h_0/d_c = 3.5$ (h_0: water depth). Velocity vertical distributions were measured by ADV along longitudinal sections across the center of boulders and between the boulders.

The calculation domain includes the complete boulder arrangement (Fig. 4). At the upstream boundary, discharge $Q = 0.127$ m^3/s is applied to match the calculated average velocity with averaged velocity measured by ADV (bulk velocity, $U_0 = 0.72$ m/s). The water depth at the downstream end is given to reproduce the experimental water depth ($h_0 = 0.193$ m) at the center of the boulder arrangement. The bed height is set to the top of the beads. The origin of the axis $x = y = z = 0$ is defined on the bed surface at the center of the boulder arrangement (x: stream-wise direction, y: leftward direction toward downstream, z: upward direction). While boulders are taken into the calculation directly as bed height undulations, the equivalent roughness height k_s and the log law origin height δz_0 are used to evaluate the resistance of the beads. The k_s and δz_0 are determined to be $k_s = 0.9\ d$ and $\delta z_0 = 0.3\ d$, using measured velocity vertical distributions on the flat rough bed without the boulders under identical flow conditions. The results of the BVC method with Non-equilibrium Wall Law (BVC-NWL) are compared with the results from the 2D calculation method and the BVC method with Equilibrium Wall Law (BVC-EWL) for flow over rough bed with boulders. In the 2D calculation method, the quadric velocity vertical distribution and hydrostatic pressure distribution are assumed with calculating equations (4)–(6). The BVC-EWL employs equations (10) and (12) without calculating momentum equations (13) and (14), assuming vertical flux across the bottom $w_{ob} = 0$. The parameters, $k_s = 0.9d$ and $\delta z_0 = 0.3d$, are the same for all three calculation methods. The drag coefficient $C_D = 0.4$ and the roughness layer thickness $\delta z_r = k_s$ are additionally given for BVC-NWL.

4 CALCULATION RESULTS AND DISCUSSION

Figure 5 shows comparisons of the velocity within the water surface and bottom horizontal planes between the ADV measurements (Papanicolaou et al., 2012) and the calculations using the 2D, BVC-EWL and BVC-NWL methods. The water surface velocity and bottom velocity were measured at $\eta = 0.1$ (highest measurement points) and 0.95, respectively. The experimental results

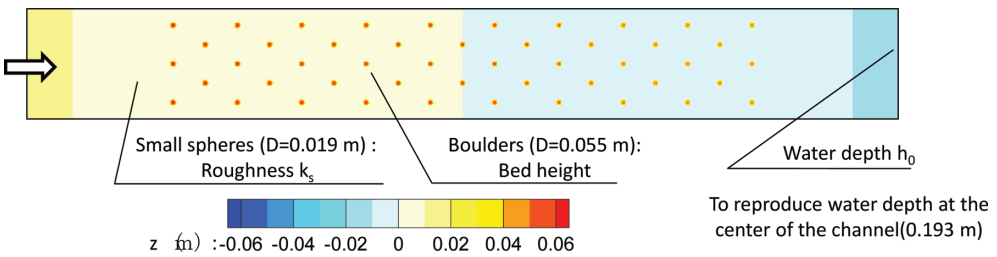

Figure 4. Calculation domains for non-equilibrium wall law.

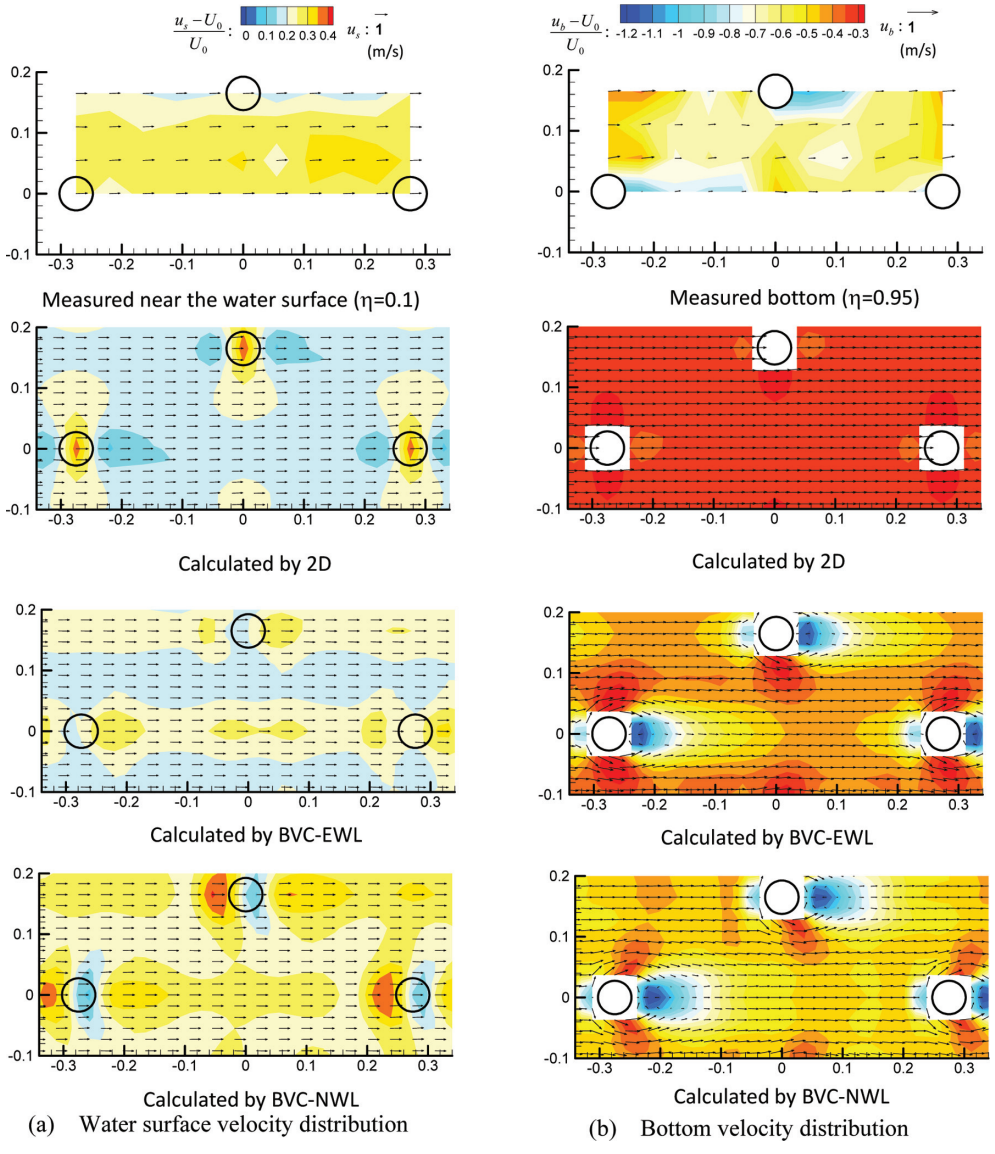

Figure 5. Water surface velocity and bottom velocity distributions (SI unit).

in Figure 5 illustrate the complex bottom velocity field with flow separations behind boulders, while the water surface flow shows a little spatial variation. All calculated water surface velocity distributions are in good agreement with the experimental results, showing almost uniform flow at the water surface, even though the 2D calculates a little lower water surface velocity than others. However, there is large difference in the calculation results for the bottom velocity distribution. Since the 2D method cannot take into account deformation in the velocity vertical distributions due to the submerged boulders, the calculated bottom velocity is almost uniform with considerable high velocity magnitude compared to the measured results. The bottom velocity by BVC-EWL captures the velocity reduction upstream of the boulders and the reverse flows in the separation zone behind them. However, the bottom velocity in-between boulders is still overestimated compared to the measured results. The bottom velocity distribution by BVC-NWL method can capture

the velocity reduction upstream and downstream of the boulders, reproducing the measured average bottom velocity. A detailed comparison of bottom velocity between the measurement and BVC-NWL shows that the calculation overestimates effects of boulders such as flow convergences beside boulders and flow separations behind them. This is attributed to the gaps between the lower surface of the boulders and the beads surface, which were not taken into account in the calculation; as the calculation bed surface is defined at the boulder top surface. Notwithstanding these differences between the experiment and calculation conditions, the calculation results provide good explanations of the experimental results.

Figure 6 shows stream-wise velocity vertical distributions along the longitudinal sections across boulders (y/d_c = 0) by measurement and calculations. The differences in calculated velocity vertical distributions between BVC-EWL and BVC-NWL are small. The complex velocity distribution of the experiment around the boulders could not be reproduced perfectly by the methods assuming a cubic velocity vertical distribution, especially for separation zone behind boulders (x/d_c = –4). The resolution of this issue requires a high-resolution vertical distribution function which needs additional momentum equations. A high-resolution three dimensional calculation method with advanced turbulence model is required for the precise calculation of flow around separation zone. However, calculation velocity vertical distributions capture the whole characteristics of those of the measurements except for local velocity variations due to the flow separation.

Figure 7 shows the velocity distributions between boulders (y/d_c = 1). We can see BVC-NWL provides a better agreement with the measurements than the BVC-EWL. In the experimental velocity distribution, the flow in the vicinity of the bed surface is disturbed due to the boulder presence which increase the mass and momentum exchange across the vortex and roughness layers. In other words, the presence of isolated boulders on rough bed increases the total resistance not only by drag force acting on the boulders but also by additional resistance acting on the bed due to the enhanced momentum exchange on bed (secondary resistance). Since BVC-EWL assumes equilibrium velocity distribution and no vertical flux, it underestimates deformations in velocity vertical distribution but overestimates the bottom velocity.

The reduction in the computational error by combining the BVC method with the non-equilibrium wall law is shown in Figure 8 for the longitudinal cross sections across (y/d_c = 0, 3) and

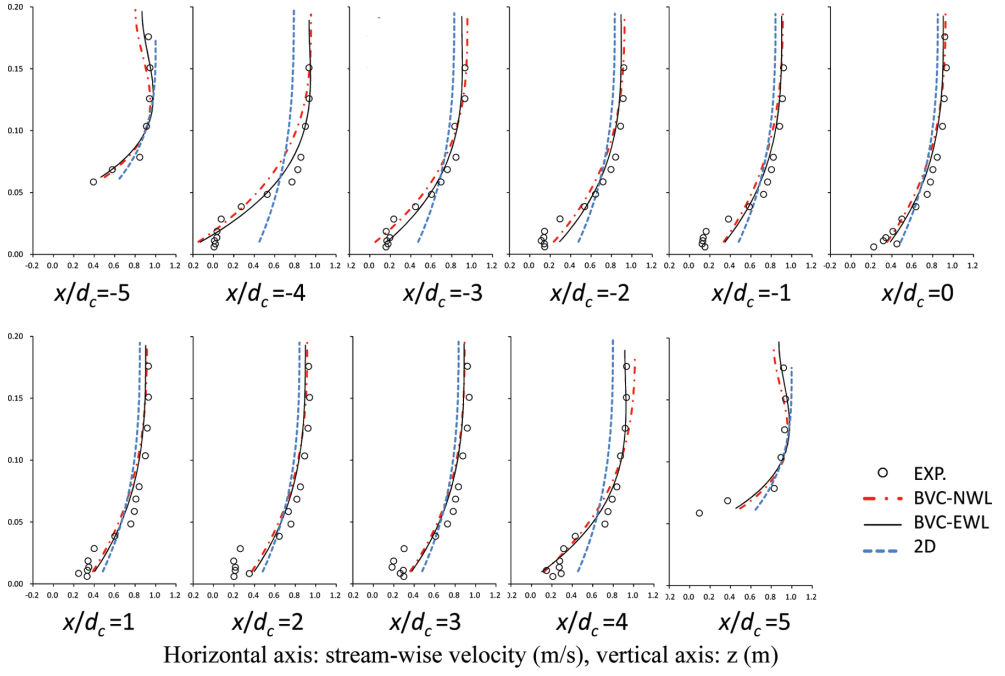

Figure 6. Stream-wise velocity vertical distribution along longitudinal section across boulders (y/dc = 0).

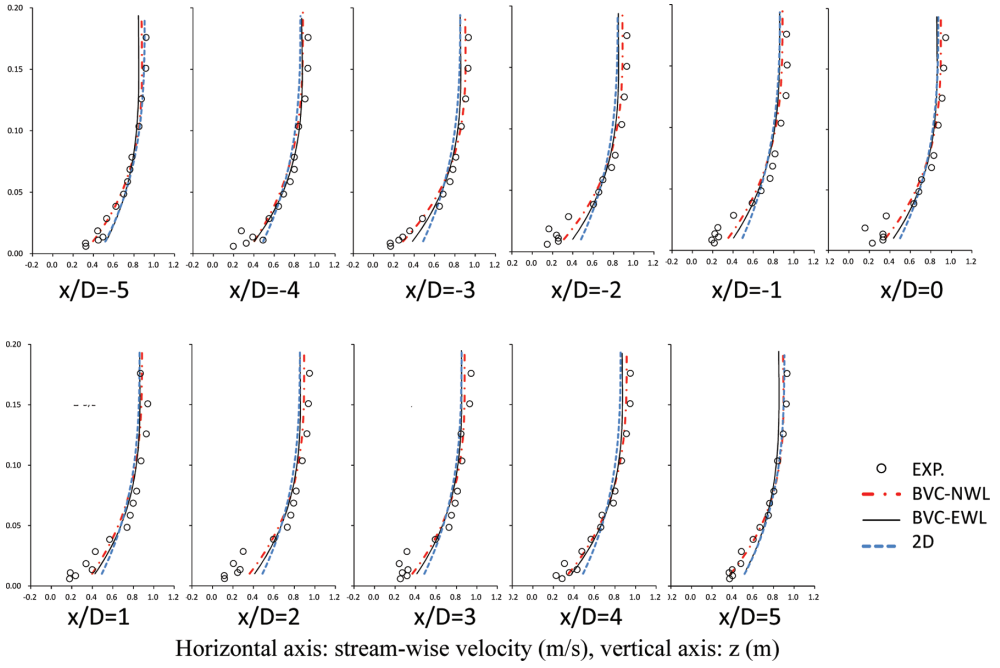

Figure 7. Stream-wise velocity vertical distribution along longitudinal section between boulders (y/dc = 1).

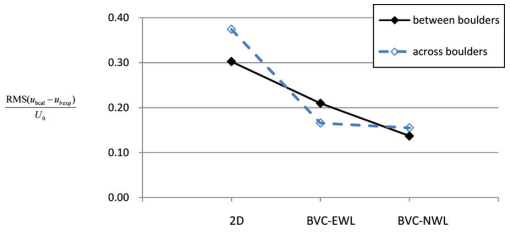

Figure 8. Calculation errors of bottom velocity by several calculation methods.

between boulders (y/d_c = 1, 2). The computational error is estimated as the root mean square of velocity difference between measured and computed results normalized by the bulk velocity U_0. The improvement by calculating vertical velocity distribution (2D—BVC-EWL) reflects the effect of the drag forces on velocity distributions, which are dominant for the line across-boulders. The error reduction for BVC-NWL compared to BVC-EWL indicates the effects of secondary resistance that the isolated boulders exert. As discussed earlier, for flow between boulders, it is important to evaluate not only the boulders drag force but also the boulders secondary effect due to the enhanced vertical momentum exchanges.

5 CONCLUSION

The non-hydrostatic quasi-3D calculation method (BVC method) with non-equilibrium wall law is proposed to calculate flow over rough bed with boulders. The present method has three calculational domains in the vertical direction in order to separate the effects of Large Scale Roughness (LSR) from that of Small Scale Roughness (SSR), namely: a main domain that takes into account the form effect of boulders, a thin vortex layer on the bed surface and a roughness layer under the bed surface. The main domain between the water surface and the vortex layer is calculated via the BVC method. For the non-equilibrium wall law, momentum and continuity equations in vortex and roughness layers are derived and solved with equations of the BVC method. Since the present method is physically based and reduces to the conventional wall law for rough bed for the uniform flow condition, we can use same parameters for the conventional equivalent wall law, such as equivalent roughness height.

The presence of isolated boulders atop a rough bed increases flow resistance not only by the drag force acting on the boulders but also by producing secondary resistance, which acts on the rough bed due to enhancing momentum exchange across the vortex and roughness layers. The BVC method can

in general take into account the drag force by calculating flows around submerged boulders. However, the BVC method with Equilibrium Wall Law (BVC-EWL) underestimates the velocity profile deformations especially in-between boulders, which is not the case when the Non-equilibrium BVC method (BVC-NWL) is used. The BVC method with Non-equilibrium Wall Law (BVC-NWL) demonstrates the ability to calculate velocity distribution over rough bed reach with isolated boulders.

REFERENCES

Aguirre-Pe, J. & Fuentes, R. 1990. Resistance to flow in steep rough streams, *Journal of Hydraulic Engineering* 116(11): 1374–1387.

Bathurst, J.C. 1985. Flow resistance estimation in mountain rivers, *Journal of Hydraulic Engineering* 111(4): 625–643.

Carney, S.K., Bledsoe, B.P. and Gessler, D. 2006. Representing the bed roughness of coarse-grained streams in computational fluid dynamics, *Earth Surface Processes and Landforms* 31(6): 736–749.

Clifford, N.J., Robert, A. and Richards, K.S. 1992. Estimation of flow resistance in gravel-bedded rivers: A physical explanation of the multiplier of roughness length, *Earth Surface Processes and Landforms* 17(2): 111–126.

Fukuoka, S. and Uchida, T. 2013. Toward integrated multi-scale simulations of flow and sediment transport in rivers, *Journal of JSCE Ser.B1 (Hydraulic Engineering)* 69(4): II_1–II_10.

Fukuoka, S., Watanabe, A. and Nishimura, T. 1992. On the groin arrangement in meandering rivers, *Journal of Hydraulic Engineering JSCE* 443/II-18: 27–36.

Ishikawa, T., Suzuki, K. and Tanaka, M. 1986. Efficient numerical analysis of an open channel flow with secondary circulations, *Proc. of JSCE* 375/II-6: 181–189.

Jin Y.-C. and Steffler, P.M. 1993. Predicting flow in curved open channels by depth-averaged method, *J. Hydraul. Eng.* 119(1): 109–124.

Katul, G., Wiberg, P., Albertson, J. and Hornberger G. 2002. A mixing layer theory for flow resistance in shallow streams, *Water Resources Research* 38(11): 321–328.

Nicholas, A.P. 2001. Computational fluid dynamics modelling of boundary roughness in gravel-bed rivers: an investigation of the effects of random variability in bed elevation, *Earth Surf. Process. Landforms* 26: 345–362.

Nikora, V., McEwan, I., McLean, S., Coleman, S., Pokrajac, D. and Walters, R. 2007a. Double-Averaging Concept for Rough-Bed Open-Channel and Overland Flows: Theoretical Background, *J. Hydraul. Eng* 133: 873–883.

Nikora, V., McLean, S., Coleman, S., Pokrajac, D., McEwan, I., Campbell, L., Aberle, J., Clunie, D. and Koll, K. 2007b. Double-Averaging Concept for Rough-Bed Open-Channel and Overland Flows: Applications, *J. Hydraul. Eng* 133: 884–895.

Olsen, N.R.B. and Stokseth, S. 1995. Three-dimensional numerical modelling of water flow in a river with large bed roughness, *Journal of Hydraulic Research*, 33(4): 571–581.

Papanicolaou, A.N., C.M. Kramer, A.G. Tsakiris, T. Stoesser, S. Bomminnayuni, and Z. Chen. 2012. Effects of a fully submerged boulder within a boulder array on the mean and turbulent flow fields: Implications to bedload transport, *Acta Geophysica*. 60(6): 1502–1546.

Rameshwaran, P., Naden, P. and Lawless, M. 2011. Flow modeling in gravel-bed rivers: rethinking the bottom boundary condition, *Earth Surf. Process. Landforms* 36: 1350–1366.

Shlichting, H. and Gersten, K. 2000. Boundary Layer Theory, 8th Revised and Enlarged Edition, Springer, Verlag Berlin Heidelberg.

Uchida, T. and Fukuoka, S. 2011. A bottom velocity computation method for estimating bed variation in a channel with submerged groins, *Journal of JSCE*, *Ser. B1* (*Hydraulic Engineering*) 67(1): 16–29.

Uchida, T. and Fukuoka, S. 2012. Bottom velocity computation method by depth integrated model without shallow water assumption, *Journal of Japan Society of Civil Engineers*, *Ser. B1* (*Hydraulic Engineering*) 68(4): I_1225–I_1230.

Uchida, T. and Fukuoka, S. 2013. Quasi 3D numerical simulation for flow and bed variation with various sand waves, *Advances in River Sediment Research*, *Proceedings of 12th International Symposium on River Sedimentation*, *ISRS*, Kyoto, Japan: 221–229.

Yeh, K.-C. and Kennedy, J.F. 1993. Moment model of nonuniform channel-bend flow. I: Fixed beds, *J. Hydraul. Eng.* 119(7): 776–795.